0026-895X/94/051055-06$03.00/0

MOLECULAR PHARMACOLOGY, 45:1055-1060

Block of the Rat Brain IIA Sodium Channel α Subunit by the Neuroprotective Drug Riluzole

TERENCE HEBERT, PIERRE DRAPEAU, LAURENT PRADIER, and ROBERT J. DUNN

Centre for Research in Neuroscience, McGill University, and Montreal General Hospital Research Institute, Montreal, Canada H3G 1A4 (T.H., P.D., R.J.D.), Department of Medical Genetics, University of Toronto, Toronto, Canada M5S 1A8 (T.H.), and Department of Molecular Neurobiology, Rhône-Poulenc Rorer S.A., 94403 Vitry sur Seine, France (L.P.)

Received November 8, 1993; Accepted March 3, 1994

SUMMARY

The effects of riluzole, a novel neuroprotective drug with anticonvulsant and anti-ischemic properties, were studied on currents carried by cloned rat brain IIA sodium channel α subunits expressed in *Xenopus* oocytes. (i) When the oocytes were held at strongly hyperpolarized potentials to close the sodium channels and riluzole was added to the external solution, the current elicited by test depolarizing pulses was reduced within a few minutes and recovered upon washout of the riluzole. Although the currents were reduced, riluzole did not shift the peak current-voltage relationship. An inhibitory constant of 30 μM was estimated for the low affinity block of closed channels. (ii) Riluzole did not affect the time course of inactivation, and repetitive stimulation at frequencies that did not result in significant accumulation of inactivation did not affect current block. These results suggest that riluzole did not block open channels. (iii) Riluzole increased steady state inactivation by shifting its voltage dependence in the hyperpolarizing direction, by prolonging the recovery from inactivation, and by blocking more effectively at high stimulation frequencies. According to the modulated receptor theory, these results suggest that riluzole binds selectively to inactivated channels, with an inhibitory constant estimated at 0.2 μM. These results show that the riluzole binding site is on the α subunit of the sodium channel, and they suggest that stabilization of the inactivated state may underlie the neuroprotective properties of riluzole.

Ischemia and hypoxia are leading causes of neurological disability and death (1). Riluzole (2-amino-6-trifluoromethoxybenzothiazole) is a novel neuroprotective agent with anti-ischemic properties in experimental animal models of these clinically important disorders (2, 3). Riluzole was first described as an anticonvulsant (4, 5), suggesting that it is a neuroprotective agent with a broad spectrum of actions and therefore is of interest for the treatment of epilepsy and ischemia (2).

The cellular pathogenesis in ischemia is thought to be mediated by the excitotoxic effects of excitatory amino acids, in particular glutamate, released as a consequence of high levels of neuronal discharge (6–8). The initial expectation was that riluzole acted as a glutamate antagonist, but the drug was not found to interfere with binding of radioactive ligands to any of the known glutamate receptor subtypes (9, 10). However, riluzole can block the activation of *N*-methyl-D-aspartate and (*RS*)-α-amino-3-hydroxy-5-methylisoxazole-4-propionic acid subtypes of glutamate receptors (11), as well as glutamate release from nerve terminals (9, 10). Interaction of riluzole with voltage-dependent ion channels has also been demonstrated. At the frog node of Ranvier, riluzole at concentrations of 10 μM or more reduces sodium and potassium currents; at lower concentrations, riluzole causes a more selective block and stabilization of inactivated sodium channels (12). Interestingly, sodium channel inhibition has been correlated with postischemic neuronal protection (13–15).

If riluzole selectively blocks inactivated sodium channels in the mammalian brain, as described for the frog channels (12), then this could account for the selective stabilization of depolarized neurons and sparing of unaffected cells that is believed to underly the neuroprotective effects of this drug. However, important structural and kinetic differences, including the inactivation properties, exist between sodium channels in different preparations (16), so that the results obtained with frog nerve may not simply be extrapolated to the mammalian brain. To examine the effects of riluzole specifically on mammalian brain sodium channels in the absence of other channel types, we have tested its effects on sodium currents recorded in voltage-clamped *Xenopus* oocytes expressing the α subunit of the predominant rat brain sodium channel (RIIA) (17). Our results demonstrate a selective block of inactivated RIIA by

T.H. was supported by a studentship from the National Science and Engineering Research Council of Canada, P.D. was supported by an award from the Fonds de la recherche en santé du Québec of Canada, and the work was supported by grants from the Medical Research Council of Canada (R.J.D.) and by Rhône-Poulenc Rorer Inc.

ABBREVIATIONS: RIIA, rat brain IIA sodium channel(s); HEPES, 4-(2-hydroxyethyl)-1-piperazineethanesulfonic acid.

riluzole and support a stabilizing effect of this neuroprotective drug in the mammalian brain.

Materials and Methods

Expression of the RIIA α subunit. RIIA cDNA was linearized with *ClaI* and transcribed *in vitro* with T7 RNA polymerase, as described previously (17, 18). Individual oocytes (stage V-VI) were injected with 7 ng of mRNA. Oocytes were incubated for 2–3 days at 20° in Barth's solution [88 mM NaCl, 1 mM KCl, 0.33 mM $Ca(NO)_2$, 0.41 mM $CaCl_2$, 0.82 mM $MgSO_4$, 2.4 mM $NaHCO_3$, 10 mM HEPES, pH 7.6]. If longer incubations were required, the oocytes were incubated in modified Liebowitz's L-15 medium; 1 volume of L-15 medium (GIBCO-BRL) was mixed with 1 volume of water, supplemented with 0.735 g/liter L-glutamine and 80 mg/liter gentamicin, and buffered with 15 mM HEPES and NaOH to a pH of 7.6.

Voltage-clamp recordings. The control recording solution consisted of 96 mM NaCl, 2 mM KCl, 1.8 mM $CaCl_2$, 1 mM $MgCl_2$, and 5 mM HEPES, pH 7.5. Oocytes injected with RIIA mRNA were perfused with this solution containing riluzole at the desired concentration. Riluzole was diluted from a 1 M stock solutin prepared in 0.2% HCl. All experiments were performed at 20–22°. Sodium currents were recorded using a two-electrode voltage clamp with a virtual ground circuit (Warner Instruments, Hamden, CT). Voltage electrodes were filled with 3 M KCl, had resistances of 1–2 MΩ, and were connected to a driven shield. To improve the clamp speed (150–250-μsec rise time constants for voltage steps), current electrodes were broken to tip diameters of 15–20 μm. To prevent leakage of the electrolyte and damage to the oocytes, the tips were filled by aspiration of a 1% agarose (Pharmacia) solution containing 3 M KCl, which was allowed to solidify, and then the electrode shaft was filled with 3 M KCl; electrode resistances were ≈0.1 MΩ. The current electrodes were connected to a grounded shield. Because the uncompensated series resistance of the virtual ground current recording circuit was ≈1 kΩ, currents no larger than 7 μA were analyzed in detail, because larger currents resulted in voltage instabilities. The current signal was filtered with an eight-pole Bessel filter at a −3-dB cutoff frequency of 10 kHz (faster response time than the clamp). Linear passive and capacitive currents were eliminated by subtraction of equivalent records in the presence of 400 nM tetrodotoxin.

Sodium channels expressed in *Xenopus* oocytes have both fast and slow inactivation. Fast-mode currents, which more closely resemble native currents, could be isolated due to their rapid recovery from inactivation using the following step protocol (18a) unless indicated otherwise. The oocytes were stepped from a holding potential of −100 mV to 0 mV for 50 msec (to inactivate all channels) and then returned to −100 mV for 5 msec (to allow only fast-mode channels to recover) before currents were recorded for subsequent test depolarizations. Pulses were applied at a rate of 1 Hz, unless indicated otherwise. Current and voltage signals were acquired at a sampling frequency of 10 kHz and analyzed using a TL1-DMA interface and pCLAMP software (Axon Instruments, Burlingame, CA). Boltzmann curves were fit using Number Crunching Statistical Software (NCSS, Kaysville, UT).

Results

Effects of riluzole on RIIA activation. We tested the effects of several concentrations of riluzole on sodium currents expressed in *Xenopus* oocytes after injection of mRNA transcribed from the cDNA clone encoding the RIIA α subunit. To illustrate the effects of riluzole, we recorded inward currents elicited by depolarizing test pulses from a holding potential of −100 mV (see Materials and Methods). These currents reached peak levels within 1 msec after initiation of the pulses (Fig. 1A). Addition of riluzole at concentrations of 1–100 μM reduced, within a few minutes of application, the amplitude of the peak

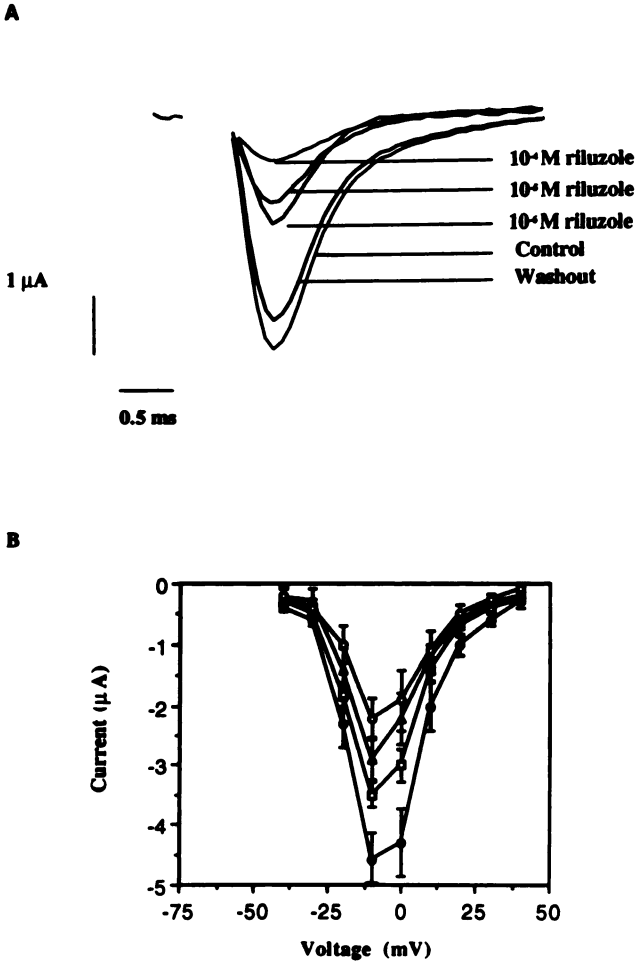

Fig. 1. Effects of riluzole on RIIA sodium currents expressed in *Xenopus* oocytes. A, Traces of RIIA currents expressed in a *Xenopus* oocyte. The oocytes were stepped from a holding potential of −100 mV to 0 mV for 50 msec and then returned to −100 mV for 5 msec before currents were recorded with a step to −10 mV for the same oocyte, in the absence and presence of 10^{-6} to 10^{-4} M riluzole. B, Current-voltage relationship for RIIA sodium current. Mean peak inward current is plotted versus test potential. Currents from oocytes treated with 10^{-4} M (○), 10^{-5} M (▲), and 10^{-6} M riluzole (□) and control currents for the same oocytes (●) (n = 5 in each case) are indicated.

sodium currents in a concentration-dependent manner. The current amplitude recovered within a few minutes of riluzole being washed out, demonstrating reversible inhibition.

Fig. 1B shows the averaged peak current-voltage relationship obtained at various riluzole concentrations. Concentrations of riluzole as high as 100 μM had no effect on the shape of the current-voltage relationship (Fig. 1B), indicating that riluzole did not affect voltage-dependent activation of the channels.

Effects of riluzole on RIIA inactivation. To test for an effect of riluzole on the rate of inactivation, the time course observed at different test potentials in the presence and absence of riluzole (10 μM) was fit with a monoexponential function. The time constants of inactivation calculated from these fits are plotted as a function of the test potential in Fig. 2 and show that riluzole had no effect on the time course of inactivation. Repetitive pulses at frequencies (10 Hz or less) that did not result in significant accumulation of inactivation did not increase the block by riluzole (Fig. 3).

In contrast to its lack of effect on the onset of inactivation,

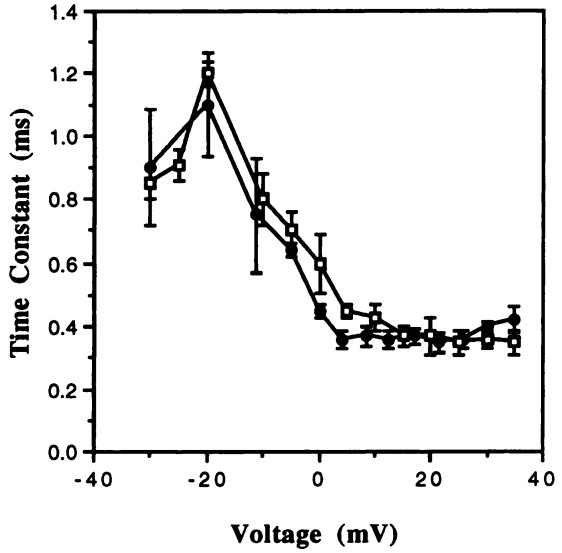

Fig. 2. Effect of riluzole on the time course of inactivation. Time constants were determined by fitting exponential functions to the decay phase of current traces elicited by test pulses to −15 mV (as described in the legend to Fig. 1), of the form $I(t) = I_0\exp(-t/\tau)$, where I_0 is the current corrected for inactivation (see Materials and Methods) and τ is the time constant of fast inactivation. Values of the time constants determined in the absence (●) and presence (□) of 10 μM riluzole are shown. The time constants are plotted as a function of test potential. Values are means ± standard deviations, unless these values were smaller than the symbols ($n = 5$ for both determinations).

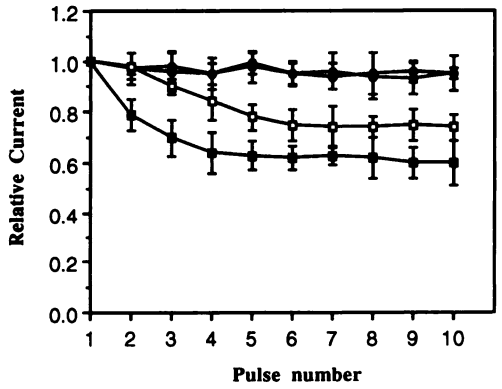

Fig. 3. Stimulation frequency dependence of riluzole block. Oocytes were held at a potential of −100 mV and were repetitively stimulated with 5-msec test pulses to −15 mV at a frequency of 10 Hz (*circles*) or 50 Hz (*squares*), in the absence (*open symbols*) or presence (*closed symbols*) of 1 μM riluzole. The peak amplitudes and standard errors ($n = 5$) of the currents elicited by each of 10 successive pulses were normalized to that observed for the first pulse.

riluzole prolonged the time course of recovery from inactivation (measured using a twin-pulse protocol), as shown in Fig. 4. Although the recovery of RIIA from inactivation in the absence of riluzole is accelerated at hyperpolarized potentials (19), recovery in the presence of riluzole was not noticeably voltage dependent (data not shown). At high stimulation frequencies (e.g., 50 Hz), the peak currents gradually decreased to a steady level due to accumulation of inactivation (Fig. 3), and exposure to riluzole (1 μM) further reduced the current levels, demonstrating use-dependent block.

When oocytes were held at depolarized potentials, riluzole application resulted in a proportionally lower current elicited by depolarizing test pulses, causing a hyperpolarizing shift of

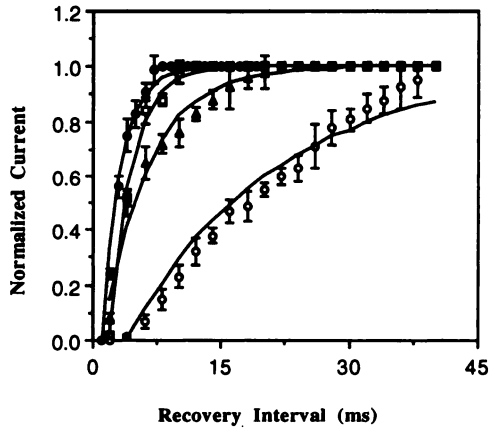

Fig. 4. Effect of riluzole on the recovery from inactivation. Recovery of currents was assayed using a two-pulse protocol in which both pulses were 50 msec in duration, to a voltage of −15 mV, and were separated by a return to the holding potential of −100 mV for the interval indicated. The peak current, relative to that seen after 40 msec, is plotted for each interval at varying riluzole concentrations [○, 10 μM ($n = 4$); △, 1 μM ($n = 4$); □, 0.1 μM ($n = 4$); ●, control currents (no drug, $n = 5$)]. Data are means ± standard errors and the fits are the means of single-exponential functions used to determine the time constants of recovery in each experiment, which were 2.6 ± 0.2 msec (●), 3.2 ± 1.4 msec (□), 6.5 ± 1.6 msec (△), and 17.5 ± 2.3 msec (○).

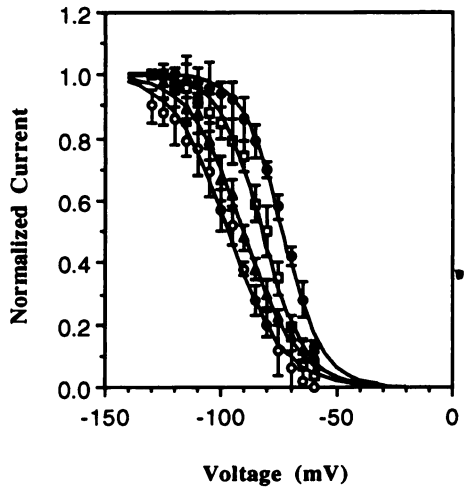

Fig. 5. Effect of riluzole on steady state inactivation. A three-pulse protocol was used to measure steady state inactivation of isolated fast-mode currents, as follows: (i) channels were inactivated with a 50-msec pulse to 0 mV, (ii) the membrane potential was stepped to various prepulse voltages for 20 msec to allow only fast-mode channels to recover, and (iii) a test pulse to 0 mV was elicited. Oocytes were exposed to riluzole concentrations of 10 μM ($n = 4$) (○), 1 μM ($n = 4$) (△), or 0.1 μM ($n = 4$) (□) or no drug (control currents, $n = 5$) (●). Data are means ± standard errors. *Solid lines*, two-state Boltzmann fits of the data to the equation $I/I_{max} = 1/[1 + \exp(V - V_{0.5})/A_h]$, where $V_{0.5}$ is the voltage for half-maximal inactivation and A_h is the number of millivolts required to produce an *e*-fold change in steady state inactivation. The values of the parameters are listed in Table 1.

the steady state inactivation curve that was dependent on the riluzole concentration (Fig. 5; Table 1). Interestingly, even a very low riluzole concentration (0.1 μM) significantly shifted the inactivation curve. This suggests that riluzole increased inactivation at all potentials by high affinity block of inactivated channels (see below).

TABLE 1

Effects of riluzole on the steady state inactivation parameters

Values are means ± standard deviations (n = 5) for the Boltzmann parameters A_h (millivolts required for an e-fold change) and $V_{0.5}$ (voltage for half-maximal inactivation) obtained for fits of the steady state inactivation data; $\Delta V_{0.5}$ is the shift in this parameter relative to the control value.

Riluzole concentration	A_h	$V_{0.5}$	$\Delta V_{0.5}$
	mV	mV	mV
Control	7.2 ± 0.6	−73.1 ± 1.2	
0.1 μM	7.5 ± 0.2	−77.1 ± 1.2*	−4.0*
1 μM	9.0 ± 1.2*	−81.9 ± 0.8*	−8.8*
10 μM	11.9 ± 0.9*	−96.5 ± 1.5*	−23.4*
Wash	8.0 ± 0.8	−75.5 ± 2.5	−2.4

* Value significantly different ($p < 0.05$, Student's t test) from that for the control set.

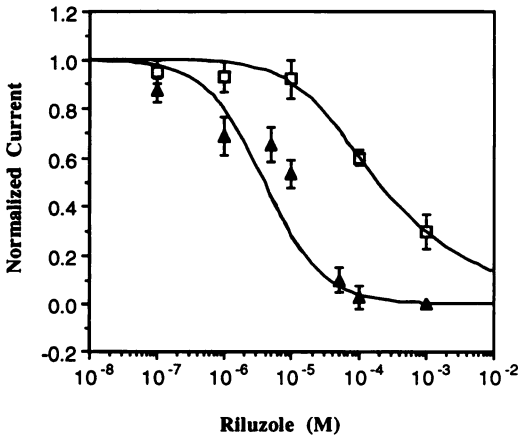

Fig. 6. Dose-response curves for the effects of riluzole on isolated fast sodium currents. Peak currents were measured in steps (see legend to Fig. 1) from a holding potential of −100 mV (n = 6) (▲), in some cases preceded by a large negative prepulse to −140 mV for 1 sec (n = 5) (□). Data are means ± standard errors. The continuous curves were calculated according to eqs. 1 and 3, as described in the text.

To estimate whether riluzole could block closed channels, the oocytes were hyperpolarized to −140 mV to ensure that inactivation was completely removed (Fig. 6). Sodium currents were then elicited by a depolarizing test pulse and the dose-response curve for riluzole inhibition was determined by testing the effects of various drug concentrations. As shown in Fig. 6, after the hyperpolarizing pulse the peak current amplitudes observed in the presence of riluzole (I_R), relative to control currents in the absence of drug (I_{ctl}), decreased as the riluzole concentration ([R]) was increased and could be fit by a saturating function:

$$I_R/I_{ctl} = [1/(1 + K_C[R])]^n \quad (1)$$

with a Hill coefficient (n) of 0.6 and an inhibitory constant (K_C) estimated at 30 μM. These results suggest a low affinity block of closed (noninactivated) channels at sites with reduced affinity at higher concentrations.

Discussion

Selective block of inactivated channels. Our results suggest that high concentrations (>10 μM) of riluzole block closed (noninactivated) RIIA channels, whereas low concentrations preferentially block inactivated channels. The conformation-selective block by riluzole is formally similar (12) to the block of sodium channels by local anesthetics proposed in the "modulated receptor" model (20, 21). Accordingly, the interactions of riluzole with the channel can be summarized by the following simplified state diagram:

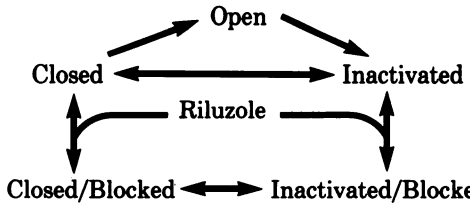

This model makes the simplifying assumption that single closed and inactivated states of the channel bind riluzole. Nonetheless, it is consistent with several key observations, namely (i) the lack of effect of riluzole on the time course of inactivation, (ii) the lack of use-dependent block of open channels at low stimulation frequencies (i.e., for which inactivation did not accumulate), (iii) the use-dependent block observed at high stimulation frequencies, and (iv) the prolonged (voltage-independent) recovery from inactivation of blocked channels. The time course and components of the recovery from inactivation for blocked channels are a function of the rate constants for several of the transitions shown in the model and are thus not simply related to the riluzole binding steps (see Ref. 22). Although we could not estimate the riluzole dissociation constant for block of inactivated channels from the kinetics of the recovery from inactivation, we were able to obtain estimates from the steady state observations.

To estimate the affinity of riluzole for inactivated channels, the shifts in the mid-points of the steady state inactivation curves obtained in the presence of riluzole ($\Delta V_{0.5}$) (see Fig. 5 and Table 1) were used to calculate the inhibitory constant for riluzole binding to the inactivated state (K_i), according to the following equation (23):

$$K_i = [R]/[(1 + [R]/K_C)/\exp(\Delta V_{0.5}/A_h) - 1] \quad (2)$$

where [R] is the riluzole concentration, K_C = 30 μM (from eq. 1), and A_h = 7.2 mV, i.e., the slope factor for the Boltzmann fit to the control data in Fig. 5. The value of K_i was estimated at 0.2 ± 0.1 μM, 150-fold lower than the value estimated for K_C, demonstrating a highly selective block of inactivated channels. This model assumes that A_h is constant, whereas it was observed to increase with the riluzole concentration. The altered voltage dependence of inactivation in the presence of riluzole may be related to more complicated interactions than those assumed in the simple state diagram presented above. As a separate measure of the relevance of this estimate of K_i, we fit the dose-response data obtained at a holding potential of −100 mV (Fig. 6), at which more inactivation was present than at −140 mV for the estimate of K_C described above, with the following equation incorporating terms for both forms of channel block (24):

$$I_R/I_{ctl} = 1/\{1 + (h_\infty \times [R]/K_C) + [(1 - h_\infty) \times [R]/K_i]\} \quad (3)$$

where h_∞ = 0.9, according to the Boltzmann fit for the data obtained in the absence of riluzole (Fig. 5). The approximation of this fit to the data is consistent with a more selective block of inactivated RIIA by riluzole.

Our results are similar to previous findings at the frog node of Ranvier (12), in which affinity constants of 90 μM and 0.29 μM were estimated for closed and inactivated sodium channels,

repectively. The several hundred-fold greater affinity estimated for riluzole binding to the inactivated state of the channels is one of the most specific state-dependent drug affinities reported. In our study only α subunit mRNA was injected into the oocytes, demonstrating that riluzole binding does not require the presence of other subunits of the sodium channel.

Relevance to neuroprotection. We observed that riluzole block of the sodium current was potentiated at high stimulation frequencies, i.e., the block was use-dependent. Riluzole is thus expected to preferentially block depolarized-hyperactive neurons in seizure loci and around ischemic zones of quiescent cells because their sodium channels are more often in the inactivated state compared with the sodium channels of normal neurons. Because selective inhibition of hyperactive neurons is the preferred manner of seizure control (25), these results argue strongly for the development of riluzole and its derivatives as a new class of neuroprotective drugs.

By acting preferentially on neurons in a depolarized state, such as during seizures or ischemia, and preventing them from additional firing and depolarizing, riluzole could have the added advantage of not interfering with normal cellular electrical activity, avoiding undesirable side effects (such as cardiac arrhythmias) of channel blockade observed with other compounds such as benzocaine and charged local anesthetics (26–30). Compounds that have effects similar to those of riluzole on steady state inactivation and recovery have been described, including neutral benzocaine (24, 31), diphenylhydantoin (32), and tocainide (33). However, these compounds have lower affinities for the inactivated state than does riluzole, which provides its advantage as a neuroprotective drug.

Although riluzole selectively blocked inactivated sodium channels at low concentrations, it also blocks with lower affinity both sodium and potassium channels at the frog node of Ranvier (12) and rat brain glutamate receptors (11). The lower affinity site may therefore be a nonspecific site or conformation common to a variety of ion channels, whereas the high affinity site appears to be specific for inactivated sodium channels, suggesting that the latter is the principal site at which riluzole effects its pharmacological actions. Interestingly, many drugs and toxins modify sodium channel gating properties (including inactivation), whereas blockers of potassium channels act preferentially on open channels, although some may also block closed channels (34). These observations suggest that the regions involved in inactivation are important sites for pharmacological regulation of the sodium channel. Previous studies of cloned sodium channels have identified several regions that are important for inactivation (35). The mutagenesis approach may therefore be of use in identifying the sites of interaction of riluzole and the inactivation mechanism of the sodium channel.

Acknowledgments

We thank Ms. G. Peard for typing the manuscript.

References

1. Choi, D. W., and S. M. Rothman. The role of glutamate neurotoxicity in hypoxic-ischemic neuronal death. *Annu. Rev. Neurosci.* **13**:171–182 (1990).
2. Malgouris, C., F. Bardot, M. Daniel, F. Pellis, J. Rataud, A. Uzan, J.-C. Blanchard, and P. M. Laduron. Riluzole, a novel antiglutamate, prevents memory loss and hippocampal neuronal damage in ischemic gerbils. *J. Neurosci.* **9**:3720–3727 (1989).
3. Pratt, J., J. Rataud, F. Bardot, M. Roux, J.-C. Blanchard, P. M. Laduron, and J.-M. Stutzmann. Neuroprotective actions of riluzole in rodent models of global and focal ischemia. *Neurosci. Lett.* **140**:225–230 (1992).
4. Benavides, J., J. C. Camelin, N. Mitrani, F. Flamand, A. Uzan, J. J. Legrand, C. Gueremy, and G. Le Fur. 2-Amino-6-trifluoromethoxy benzothiazole, a possible antagonist of excitatory amino acid neurotransmission. II. Biochemical properties. *Neuropharmacology* **24**:1085–1092 (1985).
5. Mizoule, J., B. Meldrum, M. Mazadier, M. Croucher, C. Ollat, A. Uzan, J.-J. Legrand, C. Gueremy, and G. Le Fur. 2-Amino-6-trifluoromethoxy benzothiazole, a possible antagonist of excitatory amino acid neurotransmission. I. Anticonvulsant properties. *Neuropharmacology* **24**:767–773 (1985).
6. Rothman, S. M. Synaptic release of excitatory amino acid neurotransmitter mediates anoxic neuronal death. *J. Neurosci.* **4**:1884–1891 (1984).
7. Meldrum, B. Excitatory amino acids and anoxic/ischemic brain damage. *Trends Neurosci.* **8**:47–48 (1985).
8. Rothman, S. M., and J. W. Olney. Glutamate and the pathophysiology of hypoxic-ischemic brain damage. *Ann. Neurol.* **19**:105–111 (1986).
9. Cheramy, A., R. Romo, G. Godeheu, P. Baruch, and J. Glowinski. *In vivo* presynaptic control of dopamine release in the cat caudate nucleus. II. Facilitatory or inhibitory influence of L-glutamate. *Neuroscience* **19**:1088–1090 (1986).
10. Drejer, J., T. Honore, E. Meler, and A. Schousboe. Pharmacologically distinct glutamate receptors on cerebellar granule cells. *Life Sci.* **38**:2077–2085 (1986).
11. Debono, M.-W., J. Le Guern, T. Canton, A. Doble, and L. Pradier. Inhibition by riluzole of electrophysiological responses mediated by rat kainate and NMDA receptors expressed in *Xenopus* oocytes. *Eur. J. Pharmacol.* **235**:283–289 (1993).
12. Benoit, E., and D. Escande. Riluzole specifically blocks inactivated Na channels in myelinated nerve fibre. *Pflügers Arch.* **419**:603–609 (1991).
13. Prenen, G. H. M., G. K. Gwan, F. Postema, F. Zuiderveen, and J. Korf. Cerebral cation shifts in hypoxic-ischemic brain damage are prevented by the sodium channel blocker tetrodotoxin. *Exp. Neurol.* **99**:118–132 (1988).
14. Boening, J. A., I. D. Kass, J. E. Cottrell, and G. Chambers. The effect of blocking sodium influx on anoxic damage in the rat hippocampal slice. *Neuroscience* **33**:263–268 (1989).
15. Yamasaki, Y., K. Kogure, H. Hara, H. Ban, and N. Akaike. The possible involvement of tetrodotoxin-sensitive ion channels in ischemic neuronal damage in the rat hippocampus. *Neurosci. Lett.* **121**:251–254 (1991).
16. Neumcke, B. Diversity of sodium channels in adult and cultured cells, in oocytes and in lipid bilayers. *Rev. Physiol. Biochem. Pharmacol.* **115**:1–49 (1990).
17. Auld, V. J., A. L. Goldin, D. S. Krafte, J. Marshall, J. M. Dunn, W. A. Catterall, H. A. Lester, N. Davidson, and R. J. Dunn. A rat brain Na^+ channel α subunit with novel gating properties. *Neuron* **1**:449–461 (1988).
18. Goldin, A. L., T. Snutch, H. Lubbert, A. Dowsett, J. Marshall, V. Auld, W. Downey, L. C. Fritz, H. A. Lester, R. J. Dunn, W. A. Catterall, and N. Davidson. Messenger RNA coding for only the α subunit of the rat brain Na channel is sufficient for expression of functional channels in *Xenopus* oocytes. *Proc. Natl. Acad. Sci. USA* **83**:7503–7507 (1986).
18a. Hebert, T. A., R. Montelle, R. J. Dunn, and P. Drapeau. Voltage dependencies of the fast and slow gating modes of RIIA sodium channels. *Proc. R. Soc. Lond. (B)*, in press.
19. West, J. W., T. Scheuer, L. Maechler, and W. A. Catterall. Efficient expression of rat brain type IIA Na^+ channel α subunits in a somatic cell line. *Neuron* **8**:59–70 (1992).
20. Hille, B. Local anesthetics: hydrophilic and hydrophobic pathways for the drug-receptor reaction. *J. Gen. Physiol.* **69**:497–515 (1977).
21. Hondeghem, L. M., and B. G. Katzung. Time- and voltage-dependent interactions of antiarrhythmic drugs with cardiac sodium channels. *Biochim. Biophys. Acta* **472**:373–398 (1977).
22. Colquhoun, D., and A. G. Hawkes. Relaxation and fluctuations of membrane currents that flow through drug-operated channels. *Proc. R. Soc. Lond. B Biol. Sci.* **199**:231–262 (1977).
23. Bean, B. P., C. J. Cohen, and R. W. Tsien. Lidocaine block of cardiac sodium channels. *J. Gen. Physiol.* **81**:613–642 (1983).
24. Meeder, T., and W. Ulbricht. Action of benzocaine on sodium channels of frog nodes of Ranvier treated with chloramine-T. *Pflügers Arch.* **409**:265–273 (1987).
25. Rall, T. W., and L. S. Schleifer. Drugs effective in the therapy of the epilepsies, in *The Pharmacological Basis of Therapeutics* (A. Goodman-Gilman, L. S. Goodman, T. W. Rall, and F. Murad, eds.), Ed. 7. Macmillan Publishing Co., New York, pp. 446–472 (1985).
26. Koumi, S., R. Sato, I. Misatome, M. Mayawake, H. Okumura, and R. Katori. Disopyramide block of cardiac sodium current after removal of the fast inactivation process in guinea pig ventricular myocytes. *J. Pharmacol Exp. Ther.* **261**:1167–1177 (1992).
27. Crumb, W. J., and W. Clarkson. Characterization of the sodium channel blocking properties of the major metabolites of cocaine in single cardiac myocytes. *J. Pharmacol. Exp. Ther.* **261**:910–917 (1992).
28. White, M. S., M. M. Wolf, E. A. Swinyard, G. A. Skeen, and R. D. Sofia. A neuropharmacological evaluation of felbamale as a novel anticonvulsant. *Epilepsia* **33**:564–572 (1992).
29. Villemaire, C., P. Savard, M. Talagic, and S. Nattel. A quantitative analysis

of use-dependent ventricular conduction slowing by procainamide in anesthetized dogs. *Circulation* **85**:2255–2266 (1992).
30. Grant, A. On the mechanism of action of antiarrhythmic agents. *Am. Heart J.* **123**:1130–1136 (1992).
31. Rimmel, C., A. Watte, H. Kebler, and W. Ulbricht. Rates of block by procaine and benzocaine and procaine-benzocaine interaction at the node of Ranvier. *Pflügers Arch.* **376**:105–118 (1978).
32. Tomaselli, G. F., E. Marben, and G. Jellen. Sodium channels from human brain RNA expressed in *Xenopus* oocytes: basic electrophysiological characteristics and their modification by diphenylhydantoin. *J. Clin. Invest.* **83**:1724–1732 (1989).
33. Fakler, B., J. P. Ruppersberg, W. Spittelmeister, and R. Rüdel. Inactivation of human sodium channels and the effect of tocainide. *Pflügers Arch.* **415**:693–700 (1990).
34. Hille, B. *Ionic Channels of Excitable Membranes.* Sinauer Associates Inc., Sunderland, MA (1992).
35. Catterall, W. A. Structure and function of voltage-sensitive ion channels. *Science (Washington D. C.)* **242**:50–61 (1986).

Send reprint requests to: Pierre Drapeau, Department of Neurology, Montreal General Hospital, 1650 Cedar Avenue, Montreal, Quebec, Canada H3G 1A4.